

P1.32

AN EXAMINATION OF THE LONG-LIVED MCV OF 10-13 JUNE 2003

Thomas J. Galarneau, Jr.* and Lance F. Bosart
Department of Earth and Atmospheric Sciences
University at Albany / State University of New York
Albany, NY 12222

1. INTRODUCTION:

During the period 5-14 June 2003, a subtropical jet (STJ) was positioned from just south of Hawaii east-northeastward to the southwest United States (US), then northeastward to the North Atlantic. The STJ provided a freeway for embedded upper-level disturbances to propagate from the eastern Pacific to the south-central US. These disturbances enhanced convective development as they crossed the Rockies and encountered unstable air (Galarneau and Bosart 2004).

This active STJ period occurred during the field phase of the Bow Echo and Mesoscale Convective Vortex (MCV) Experiment (BAMEX; Davis et al. 2004). This period included 19 convective systems, including several MCVs, and four intensive operations periods (IOPs; Bosart and Galarneau 2004; Davis et al. 2004). The MCV of 10-13 June 2003, sampled by IOP 8, will be the focus of this paper.

MCVs are warm core systems (in the middle and lower troposphere) that have been documented to develop in the stratiform region of mesoscale convective systems (MCSs; e.g., Johnston 1981; Zhang and Fritsch 1987; Menard and Fritsch 1989). A cyclonic (anticyclonic) vorticity maximum is characteristically found in mid-levels (near the surface) associated with a diabatic heating maximum (lower-tropospheric cold pool). There are occasions, however, in which the cyclonic circulation reaches the surface when convective redevelopment within the MCV's circulation causes low-level heights to fall and cyclonic vorticity to grow downward (e.g., Rogers and Fritsch 2001). Although most MCVs dissipate as the parent MCS decays, there are occasions in which the MCV can last long after the parent MCS dissipates and even retrigger convection (e.g., Bartels and Maddox 1991). Davis and Weisman (1994) suggest that the longevity of MCVs may be

controlled by vertical wind shear. Weak but well-defined shear confined to low-levels appears to maximize longevity, whereas moderate shear throughout the depth of the vortex weakens the MCV. These long-lived MCVs can produce excessive rains over large regions by reorganizing convection over several diurnal heating cycles (e.g., Bosart and Sanders 1981; Menard and Fritsch 1989; Fritsch et al. 1994).

On 0000 UTC 10 June 2003, an upper-level disturbance embedded in the STJ enhanced convective development as it crossed the Rockies and encountered unstable air in eastern New Mexico and western Texas. Remnant mid-level vorticity from this convection moved northeast into Oklahoma, and organized into a MCV amidst newly formed deep moist convection (Fig. 1). The uniqueness of this MCV lies in its longevity as it penetrated to the surface and its transition into a baroclinic surface cyclone as it interacted with baroclinicity over the Great Lakes. The purpose of this paper is to examine the large-scale antecedent conditions and the structural evolution of this long-lived MCV.

2. DATA AND METHODS:

Analyses and diagnostic calculations prepared in this manuscript for the large-scale overview were derived from the 2.5° National Centers for Environmental Prediction and National Center for Atmospheric Research (NCEP/NCAR) Reanalysis (Kalnay et al. 1996; Kistler et al. 2001) and the 1.0° Global Forecast System (GFS) analyses. The 32 km North American Regional Reanalysis was used for meso- to synoptic-scale analysis of the MCV (Mesinger et al. 2005).

Satellite and radar imagery, 1-minute Automated Surface Observing System (ASOS) data and intensive operations period (IOP) 8 dropsondes were obtained from the BAMEX Field

*Corresponding author address:

Thomas J. Galarneau, Jr., Department of Earth and Atmospheric Sciences, University at Albany/SUNY, 1400 Washington Avenue, Albany, NY 12222
Email: tomjr@atmos.albany.edu

Catalog¹. Satellite imagery were also obtained from the University at Albany archives.

The coupling index (CI) is used as a proxy for atmospheric stability in this manuscript. It is defined as θ on the dynamic tropopause (DT; defined as the 1.5 potential vorticity unit (PVU) surface) minus θ_e at 850 hPa. CI values < 4 K (< 0 K) are indicative of weakly stable (convectively unstable) regions where deep moist convection could develop, given adequate moisture and lift (see Bosart and Lackmann 1995).

3. RESULTS:

a) Large-scale overview

The period 5-14 June 2003 was marked by a STJ, positioned from just east of Hawaii stretching northeastward to the North Atlantic, that was manifest by the split flow regime (ridge poleward of trough) over the eastern Pacific downstream of a large-scale trough over the central Pacific (Fig. 2). The STJ strengthens from 20 m s^{-1} over the eastern Pacific to 30 m s^{-1} over the contiguous US in a region of anomalous southwesterly flow poleward (equatorward) of anomalously high (low) heights over the western Atlantic (northern Great Plains).

Four equally spaced upper-level disturbances (A through D) embedded in the STJ by 0000 UTC 9 June 2003 (00Z/09) originated from transient meso- to synoptic-scale disturbances within the aforementioned large-scale trough in the eastern Pacific (Fig. 3). Disturbances A, C and D broke off from trailing vorticity filaments that reached south of 30°N between 140°W and 160°W at 00Z/04, 00Z/07 and 00Z/09, respectively. These disturbances moved eastward along the axis of the STJ. Disturbance B originated from a meso-scale transient disturbance that was positioned north of 30°N . In response to the northward placement relative to the other three disturbances, disturbance B moved around the poleward periphery of the downstream ridge as a "Ridge Roller" (RR; see Galarnau and Bosart 2006) over the eastern Pacific during the period 00Z/04 through 00Z/08. Disturbance B then began moving eastward by 00Z/09 when it moved far enough south to feel the effects of the STJ.

The STJ disturbances were associated with low clouds while over the eastern Pacific likely due to the weakly-to-strongly stable atmosphere as indicated by a $\text{CI} > 4$ K (Fig. 4)². At 00Z/10, STJ disturbance A crossed the Rockies of Arizona and New Mexico. Diurnally forced deep moist convection was ongoing along the higher terrain of New Mexico, Colorado and Wyoming at this time². The convection along the leading edge of disturbance A became a well-organized MCS by 03Z/10 as it moved southeast toward the Gulf of Mexico. As disturbance A continued northeast toward Oklahoma, another round of convection became associated with disturbance A over central Oklahoma by 00Z/11. It is from this convection that low- to mid-level vorticity, remnants of the New Mexico/Texas MCS from 00Z-06Z/10 that moved northeastward with disturbance A, grew in scale and strengthened becoming the long-lived MCV discussed in the next section of this paper (Fig. 1)². By 12Z/11, disturbance B crossed the Rockies of New Mexico and Texas and triggered convection farther east over central Texas at 00Z/12². The convection was triggered farther east, when compared to disturbance A, because the weakly stable to convectively unstable air ($\text{CI} < 4$ K) was displaced farther east (not shown). Disturbances C and D, became associated with convection after crossing the Rockies as well, but will not be discussed further in this paper.

b) Evolution of MCV

A weak 850-700 hPa layer-averaged absolute vorticity maximum ($\sim 12 \times 10^{-5} \text{ s}^{-1}$) developed in the stratiform region of the New Mexico/Texas MCS, associated with disturbance A, by 03Z/10 (not shown). This cyclonic vorticity center, along with disturbance A, moved northeast toward Oklahoma as the initial MCS moved southeast toward the Gulf of Mexico². By 18Z/10, the 850-700 hPa disturbance merged with remnant convectively-produced 850-700 hPa vorticity moving south from Kansas, over western Oklahoma (not shown). At 00Z/11, new convection formed in response to disturbance A and the north-south elongated 850-700 hPa vorticity center (Fig. 5a). Cross-sections of PV at 00Z/11 show the effects the newly formed convection in the ridging aloft above the low- to mid-level disturbance (Fig. 6a,b). The ridging aloft deformed disturbance A and split it into a leading

¹ BAMEX Field Catalog:
<http://www.joss.ucar.edu/bamex/catalog/index.html>

² Radar and Satellite imagery available at:
<http://www.atmos.albany.edu/student/tomjr/conflinks/conflinks.html>

“a” and trailing “A” disturbance. Leading disturbance “a” moved to the south and east and dissipated while the trailing “A” disturbance remained tied to the developing MCV. By 12Z/11, the 850-700 hPa disturbance has grown in scale and has become a well developed MCV ($\sim 32 \times 10^5 \text{ s}^{-1}$) with a circulation apparent in the radar imagery (Fig. 5b)². By 00Z/12, the MCV has grown further in the horizontal and vertical and developed a second low-level PV maximum in the 900-700 hPa layer ($\sim 1.2 \text{ PVU}$; Figs. 5c, 6c,d) while helping to trigger another round of convection on its south and east flank (downshear right; DSR)². The MCV became elongated by 12Z/12 in response to increased baroclinicity in low- to mid-levels (Figs. 5d, 7). The MCVs interaction with the low- to mid-level baroclinicity occurred in conjunction with precipitation becoming stratiform, with some banded structures, and shifting to downshear left (DSL)². As the MCV approached the Great Lakes, STJ disturbance A began to move downstream of the MCV to the south and east (Fig. 6e, f). Concurrently, the MCV began to lean downshear and weaken ($\sim 1.2 \text{ PVU}$) during the period 18Z/12–12Z/13 (Fig. 5e, f, 6e, f).

During this weakening phase, the MCV’s circulation began interacting with existing baroclinicity over the Great Lakes. The baroclinicity was present in response to cooler lake-influenced air ($\theta \sim 12^\circ\text{C}$) meeting relatively warmer air ($\theta \sim 20^\circ\text{C}$) over land. The interaction culminated with the MCV acquiring surface frontal structure by 21Z/12 through warm frontogenesis on the south side of Lake Erie and cold frontogenesis south of Lake Huron and east of Lake Michigan (not shown). Enhanced warm advection stratiform precipitation developed in association with the newly formed warm front while deep moist convection developed ahead of the cold front in the warm sector². See Galarnau and Bosart (2004) for further analysis of this transition from an MCV to a frontal cyclone.

4. DISCUSSION:

The period 5-14 June 2003 during BAMEX featured a STJ beginning just east of Hawaii stretching east-northeastward to the southwest US, the northeast to the North Atlantic. Upper-level disturbances embedded in the STJ enhanced convective development as they crossed the Rockies and encountered unstable air. These disturbances were not associated with convection west of the Rockies because of a weakly-to-strongly stable atmosphere.

A mid-level cyclonic circulation developed in the trailing stratiform region of an MCS over eastern New Mexico and western Texas that developed in association with STJ disturbance A. The mid-level disturbance moved northeast with disturbance A to Oklahoma, triggering a second MCS. The mid-level disturbance grew vertically and expanded horizontally, in the stratiform region of this new MCS, into a near tropospheric deep MCV by 12Z/11. The MCV circulation reaches the surface by 12Z/11 in conjunction with a second PV maximum developing beneath the mid-level PV maximum in the 900-700 hPa layer. The PV growth at low-levels developed in response to increased stability and absolute vorticity in the 900-700 hPa layer (Figs. 6c, 8). As the MCV approached the Great Lakes, disturbance A passed downstream to the south and east of the MCV. Subsequently, the MCV began to lean downshear and weaken. During the MCVs weakening, surface frontal structure was acquired as the MCVs circulation interacted with existing baroclinicity over the Great Lakes. This pre-existing surface baroclinicity was present through differential diabatic heating between the land surface and relatively cooler lake waters.

Twenty-three dropsondes were released between 16-19Z/11 during IOP 8. Figure 7, showing time and space corrected pressure and winds on the $\theta=310 \text{ K}$ surface, is derived from the dropsondes taken during IOP 8 and provides an opportunity to compare the mature stage of this long-lived MCV to the conceptual model of isentropic motion associated with a MCV presented in Raymond and Jiang (1990). In Fig. 7 isentropic upgliding is evident ahead of the MCV as parcels beginning in the southeast quadrant would move from higher pressure up to lower pressure (isentropic ascent) in the northeast quadrant. Isentropic downgliding is evident behind the MCV. This is upgliding/downgliding couplet is consistent with the Raymond and Jiang (1990) model of an MCV embedded within a background baroclinic zone. This MCV is also embedded within westerly shear with uplifted (downlifted) isentropes below (above), which is consistent with Raymond and Jiang (1990). This configuration of ascent places the bulk of precipitation DSL of the MCV center in the conceptual model. This is not seen initially in the long-lived MCV however, as deep moist convection was found DSR at the beginning of IOP 8. This convection formed in the DSR quadrant of the MCV in a moist, unstable and highly sheared environment, were MCV-induced

upward motion was maximized in a region of surface baroclinicity approximately 500 km from the MCV center (not shown). By 00Z/12, however, the precipitation had shifted to primarily DSL, becoming more consistent with the Raymond and Jiang (1990) conceptual model.

5. RELATED SCIENTIFIC ISSUES:

The following are considerations for further postulation on the evolution of this long-lived MCV:

- Was ambient vorticity in the lee of the Rockies present and if so, important in MCV generation as disturbance A crossed the Rockies?
- What processes led to the MCV circulation reaching the surface?
 - Downward building in response to increased Rossby penetration depth as MCV grew horizontally?
 - In situ low-level circulation growth through vorticity generation by convergence and stretching?
- During the strengthening phase of the MCV, the deep-layer shear weakens below 12.5 m s⁻¹. Did this shear weakening play an important role in MCV strengthening? Would this be a tropical cyclogenesis problem if a warm ocean (sea-surface temperature > 26°C) were beneath this MCV, rather than land?
- What processes caused the MCV to lean downshear as deep moist convection weakened?

6. ACKNOWLEDGEMENT:

This research is supported by NSF grant #ATM-0233172. Celeste Iovinella is thanked for submitting the manuscript in final form.

7. REFERENCES:

Bartels, D.L. and R.A. Maddox, 1991: Midlevel cyclonic vortices generated by mesoscale convective systems. *Mon. Wea. Rev.*, **119**, 104-118.

Bosart, L.F. and F. Sanders, 1981: The Johnstown flood of July 1977: A long-lived convective system. *J. Atmos. Sci.*, **38**, 1616-1642.

Bosart, L.F. and G.L. Lackmann, 1995: Postlandfall

tropical cyclone reintensification in a weakly baroclinic environment: A case study of Hurricane David (September 1979). *Mon. Wea. Rev.*, **123**, 3268-3291.

Bosart, L.F. and T.J. Galarneau, Jr., 2004: Subtropical jet disturbances as initiators of convection during BAMEX. *Preprints*, 26th Conference on Hurricanes and Tropical Meteorology, Amer. Meteor. Soc., 3-7 May 2004, Miami, FL, pp. 296-297.

Davis, C.A. and M.L. Weisman, 1994: Balanced dynamics of mesoscale convective vortices produced in simulated convective systems. *J. Atmos. Sci.*, **51**, 2005-2030.

Davis, C.A. and Coauthors, 2004: The bow echo and MCV experiment. *Bull. Amer. Meteor. Soc.*, **85**, 1075-1093.

Fritsch, J.M., J.D. Murphy and J.S. Kain, 1994: Warm core vortex amplification over land. *J. Atmos. Sci.*, **51**, 1780-1807.

Galarneau, T.J.Jr. and L.F. Bosart, 2004: The long-lived MCV of 11-13 June 2003 during BAMEX. *Preprints*, 22nd Conference on Severe Local Storms, Amer. Meteor. Soc., 4-8 October 2004, Hyannis, MA, **CD-ROM**, paper 5.4.

Galarneau, T.J.Jr. and L.F. Bosart, 2006: Ridge rollers: Mesoscale disturbances on the periphery of cutoff anticyclones. *Preprints*, Severe Local Storms Special Symposium, Amer. Meteor. Soc., 29 January-2 February 2006, Atlanta, GA, **CD-ROM**, paper P1.11.

Johnston, E.C., 1981: Mesoscale vorticity centers induced by mesoscale convective complexes. *Preprints*, 9th Conference on Weather and Forecasting, Amer. Meteor. Soc., Seattle, WA, pp.196-200.

Kalnay, E. and Coauthors, 1996: The NCEP/NCAR 40-year reanalysis project. *Bull. Amer. Meteor. Soc.*, **77**, 437-472.

Kistler, R. and Coauthors, 2001: The NCEP/NCAR 50-year reanalysis: monthly means CD-ROM and documentation. *Bull. Amer. Meteor. Soc.*, **82**, 247-268.

Menard, R.D. and J.M. Fritsch, 1989: An MCC-generated inertially stable warm core vortex. *Mon. Wea. Rev.*, **117**, 1237-1261.

Mesinger, F. and Coauthors, 2005: North American Regional Reanalysis. Submitted to *Bull. Amer. Meteor. Soc.*

Rogers, R.F. and J.M. Fritsch, 2001: Surface

cyclogenesis from convectively driven
amplification of midlevel mesoscale convective
vortices. *Mon. Wea. Rev.*, **129**, 605-637.

Inertially stable warm-core vortex and the
mesoscale convective complex. *J. Atmos. Sci.*,
44, 2593-2612.

Zhang, D.L. and J.M. Fritsch, 1987: Numerical
simulation of the meso- β scale structure and
evolution of the 1977 Johnstown flood. Part II:

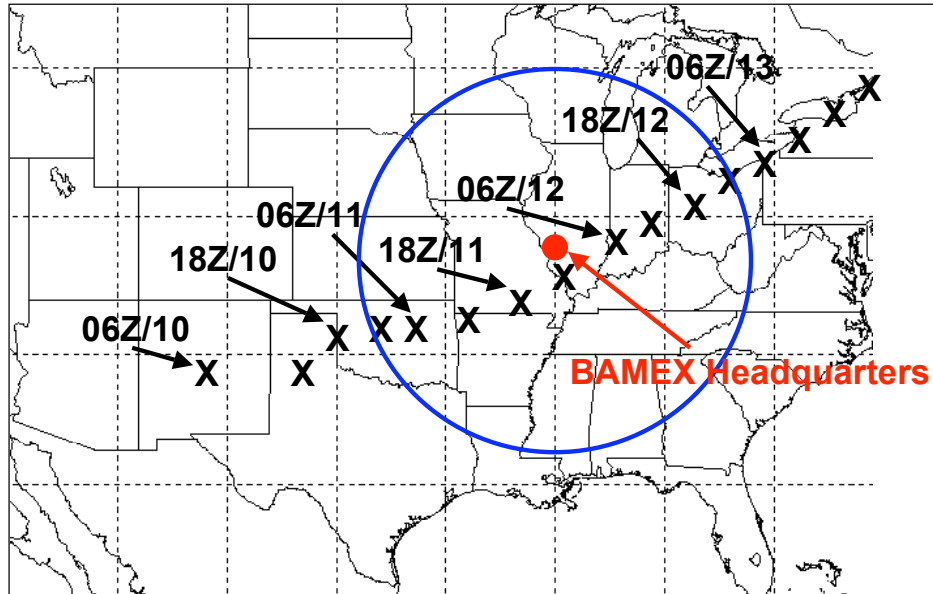


Figure 1: Track of MCV from 06Z/10 through 00Z/14 marked every 6 hours. Blue circle denotes BAMEX domain.

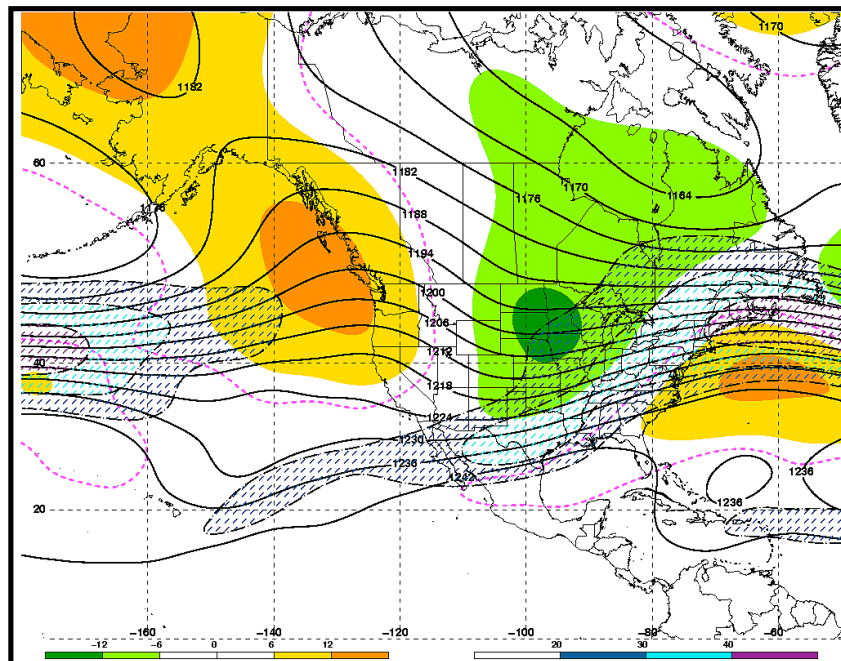


Figure 2: 200 hPa height mean (solid contours; dam) and anomaly (shaded; dam) and vector wind mean (stippled isotachs; m s^{-1}) for 5-14 June 2003. The color bar for the 200 hPa height anomalies (200 hPa isotachs) are in the lower left (right) corner. Anomaly is based upon 5-14 June long-term mean for 1968-1996. Dashed magenta contour denotes +3 dam 200 hPa height anomaly.

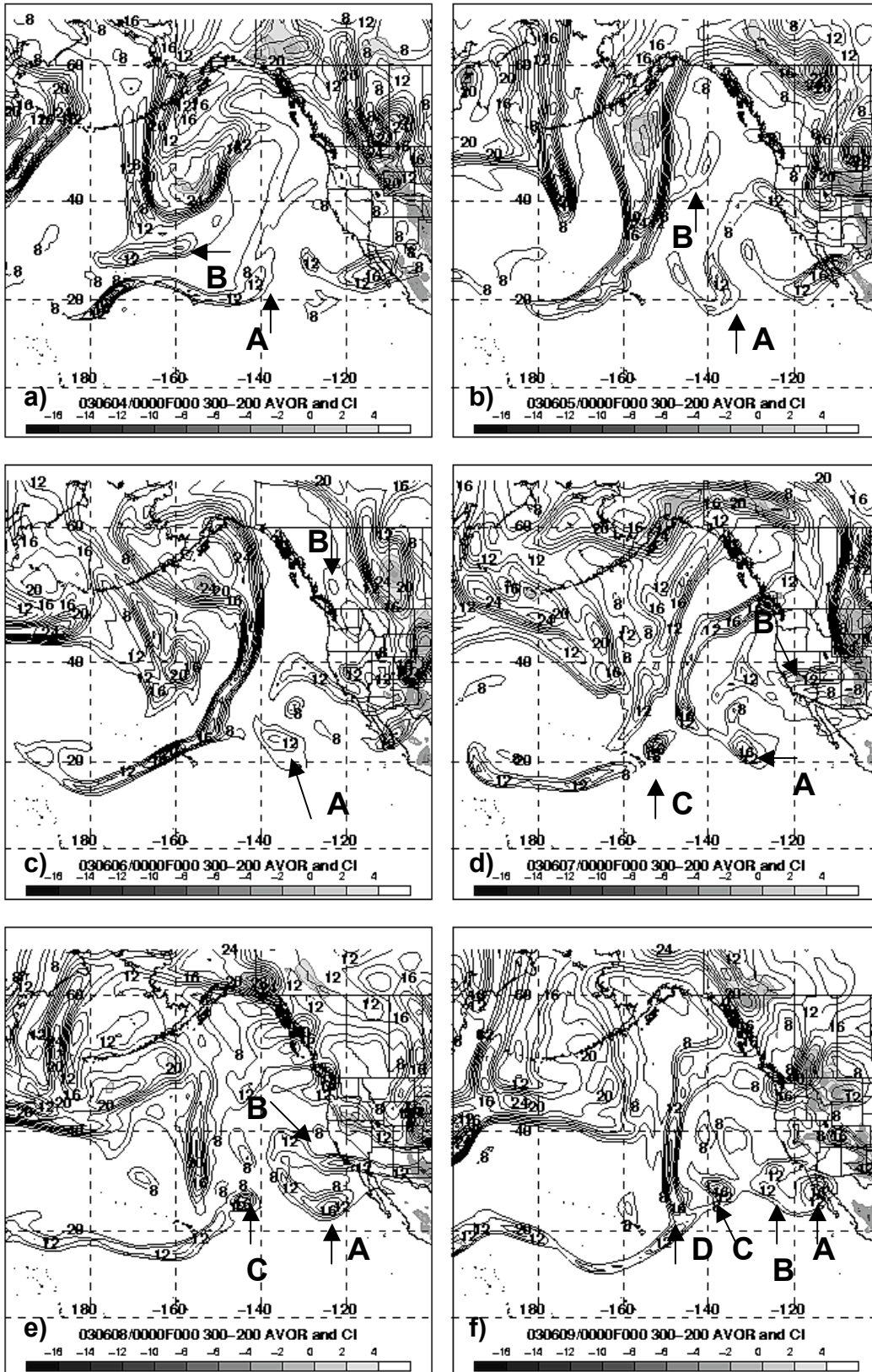


Figure 3: 300-200 hPa layer-averaged absolute vorticity (solid contours; $\times 10^{-5} \text{ s}^{-1}$) and CI (shaded $< 4 \text{ K}$) for (a) 00Z/04, (b) 00Z/05, (c) 00Z/06, (d) 00Z/07, (e) 00Z/08 and (f) 00Z/09. STJ disturbances A, B, C and D are labeled.

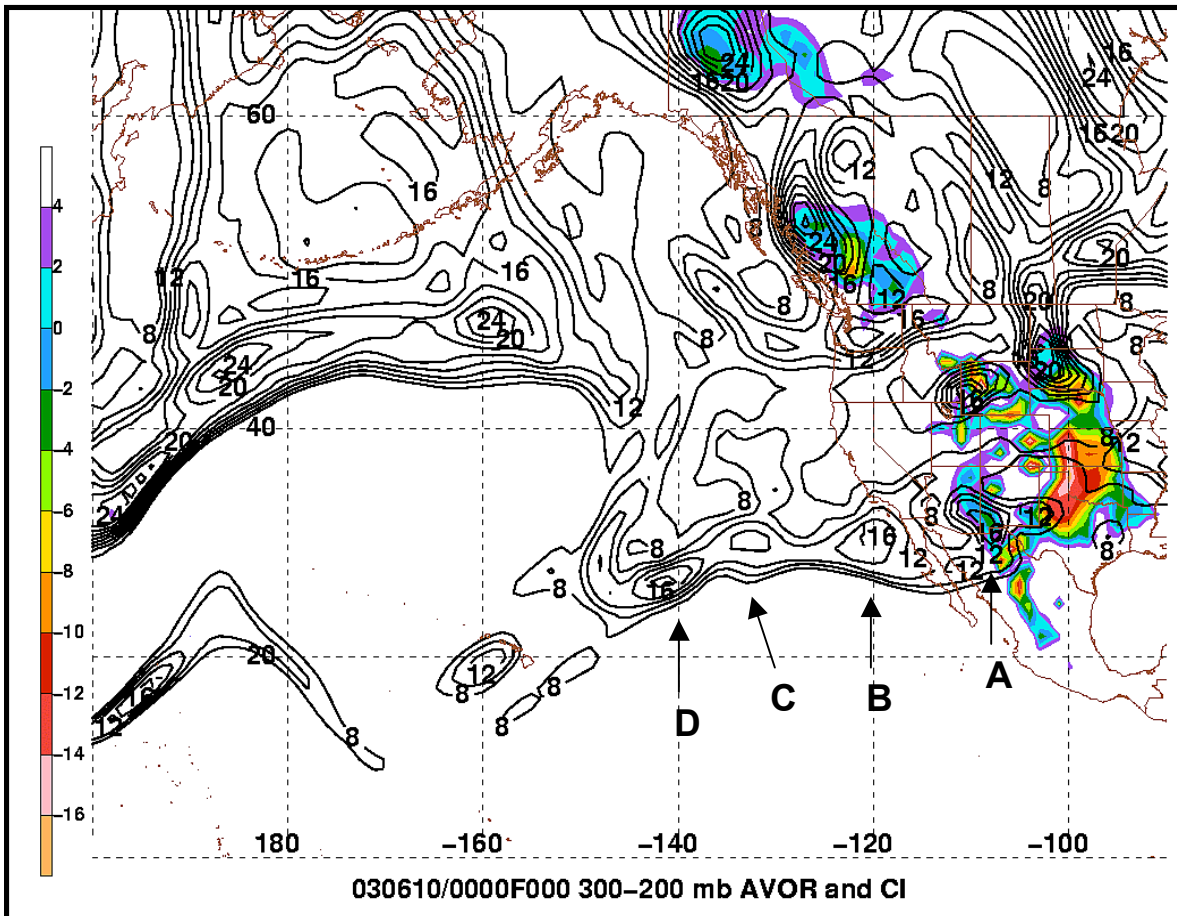


Figure 4: 300-200 hPa layer-averaged absolute vorticity (solid contours; $\times 10^{-5} \text{ s}^{-1}$) and CI (shaded; K) for 00Z/10. STJ disturbances A, B, C and D are labeled.

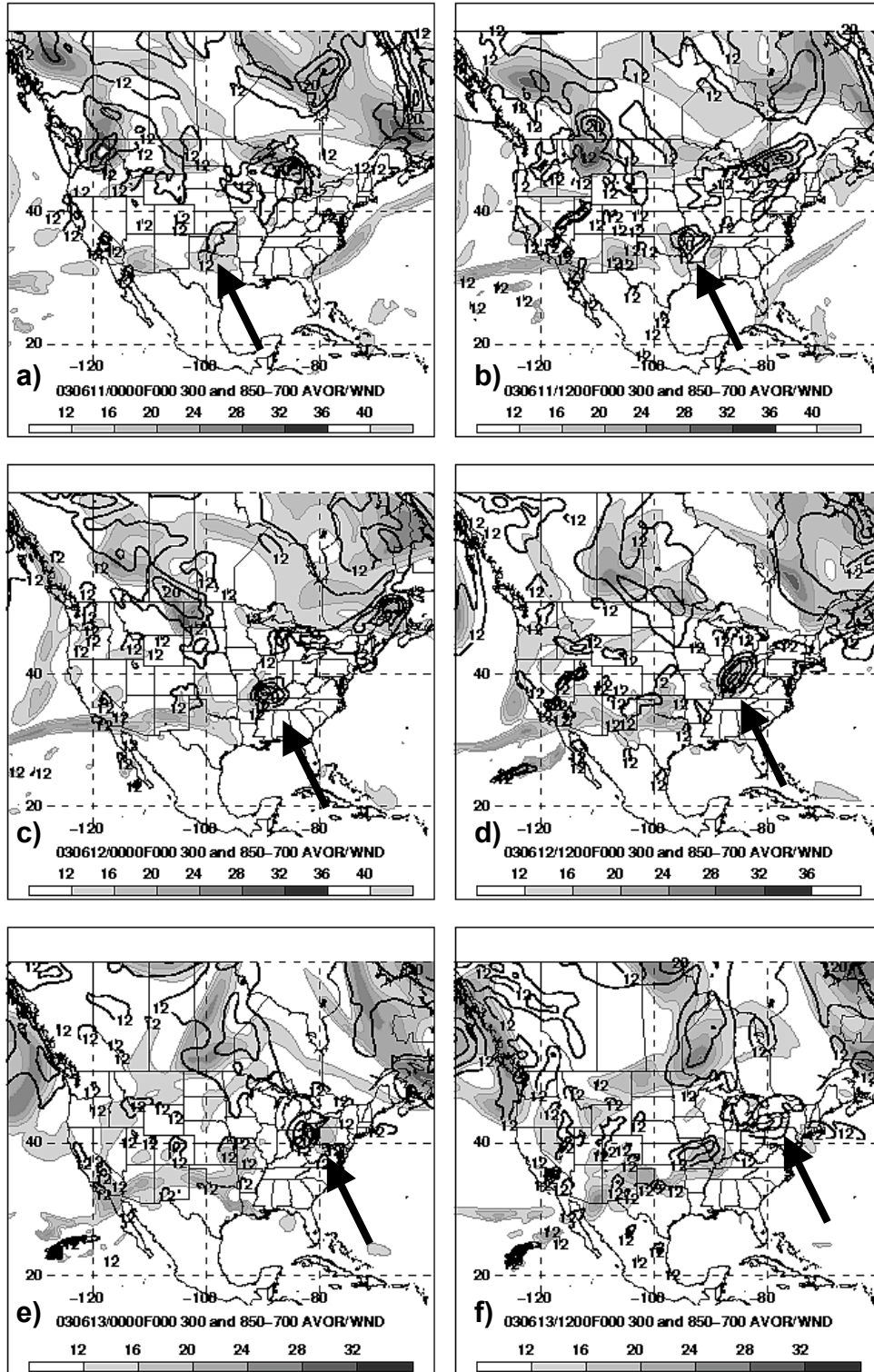


Figure 5: 300 hPa absolute vorticity (shaded grey contours; $\times 10^{-5} \text{ s}^{-1}$) and 850-700 hPa layer-averaged absolute vorticity (solid contours; $\times 10^{-5} \text{ s}^{-1}$) for (a) 00Z/11, (b) 12Z/11, (c) 00Z/12, (d) 12Z/12, (e) 00Z/13 and (f) 12Z/13. Arrows point to MCV location.

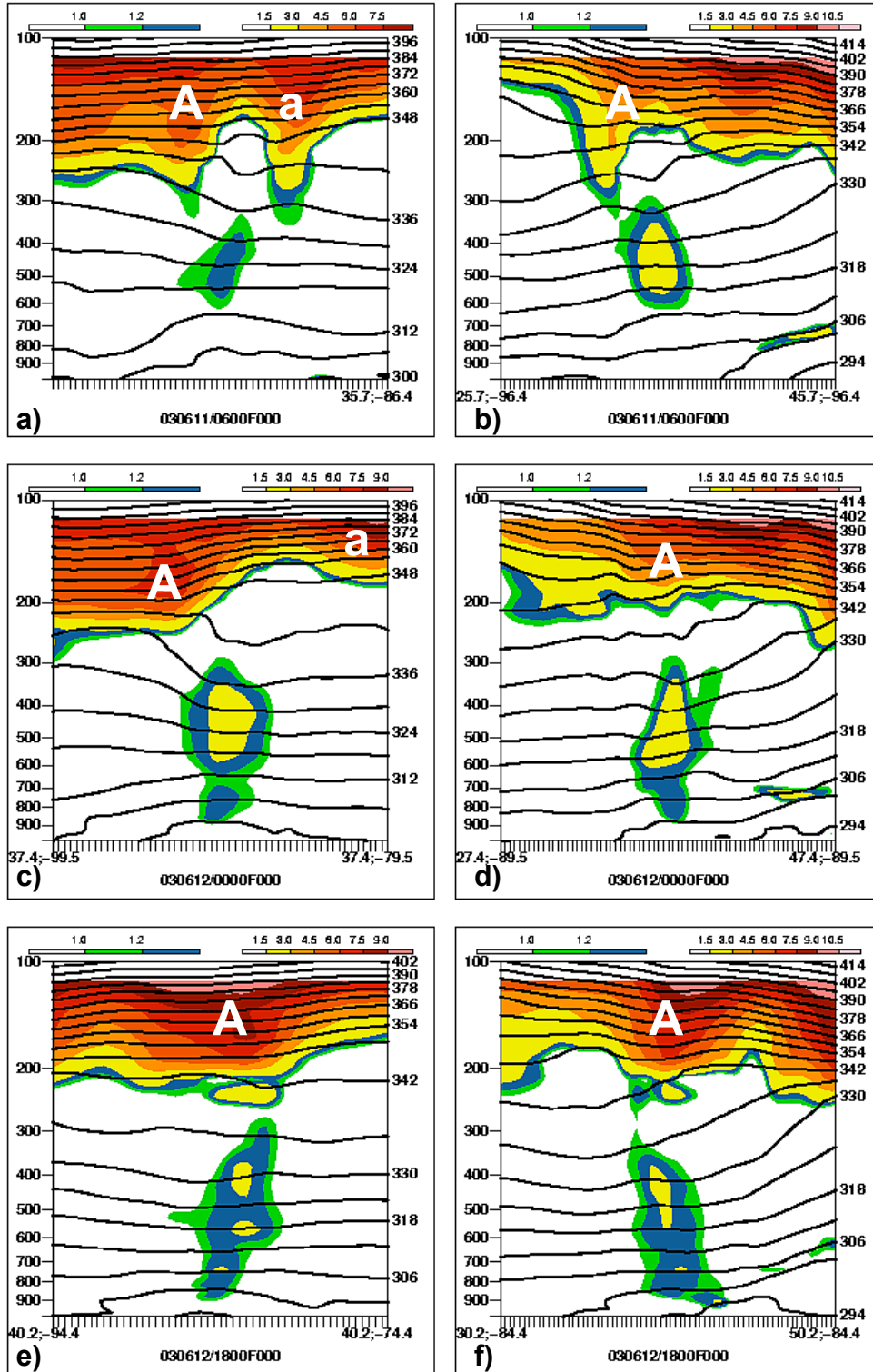


Figure 6: Cross sections of PV (shaded; PVU) and potential temperature (solid contours; K) for (a) 06Z/11 west-to-east (WE), (b) 06Z/11 south-to-north (SN), (c) 00Z/12 WE, (d) 00Z/12 (SN), (e) 18Z/12 WE and (f) 18Z/12 (SN). WE (SN) cross-sections cover 20° longitude (latitude) centered on MCV. STJ disturbances “A” and “a” are labeled.

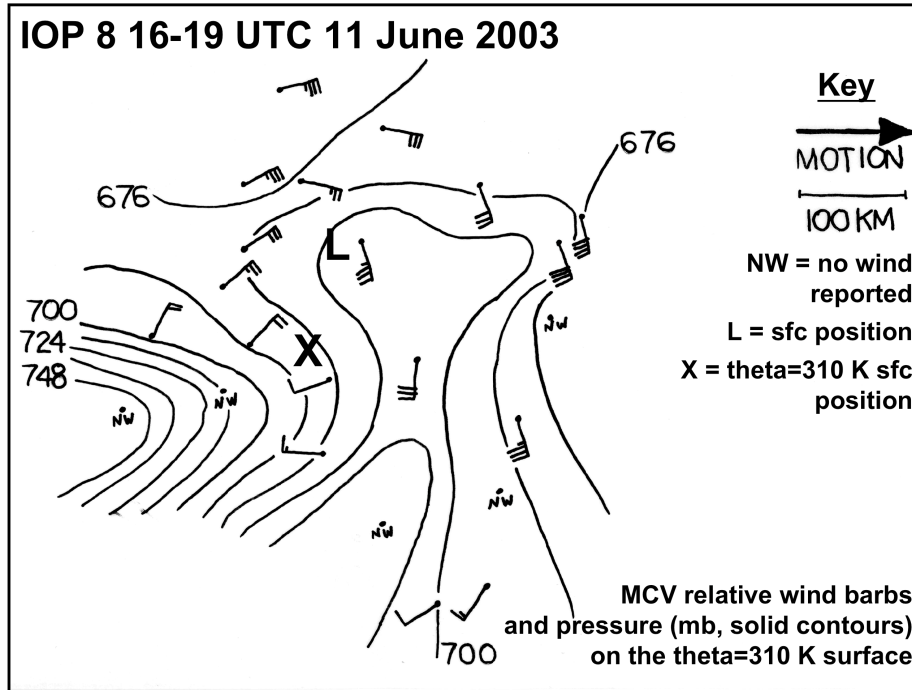


Figure 7: Time-space corrected manual analysis of pressure (solid contours; hPa) and wind (barbs; knots) on the $\theta=310$ K surface derived from the IOP 8 dropsondes. NW denotes that no wind was reported. "L" marks the surface position and "X" marks the $\theta=310$ K surface position.

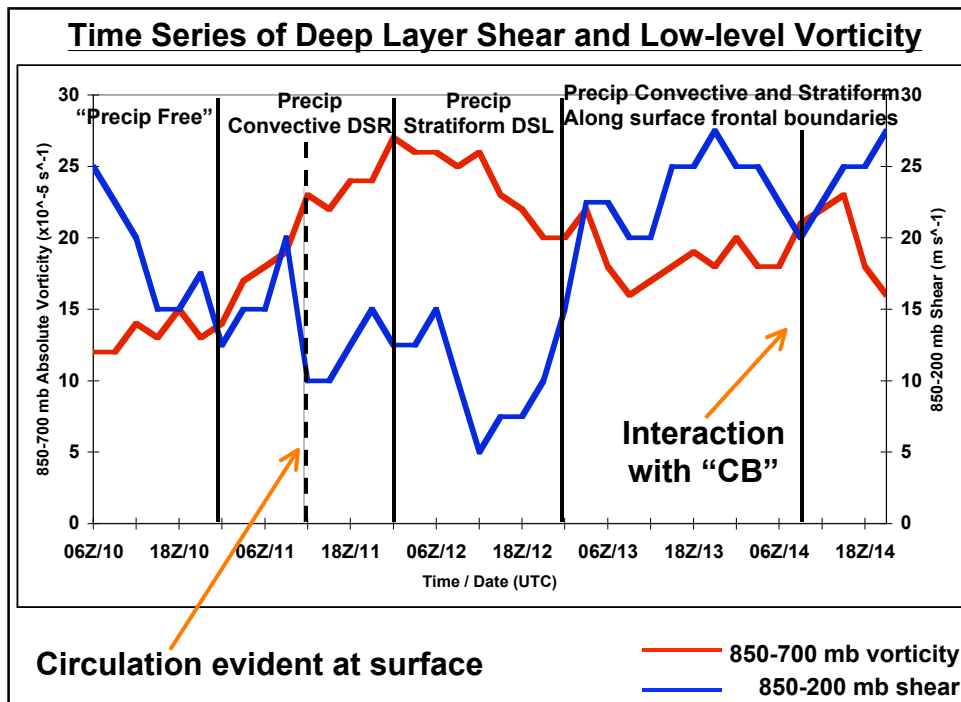


Figure 8: Time series of subjectively analyzed 850-700 hPa layer-averaged absolute vorticity (red line; $\times 10^{-5} \text{ s}^{-1}$) and 850-200 hPa wind shear (blue line; m s^{-1}).